AGU PUBLICATIONS

Paleoceanography

RESEARCH ARTICLE

10.1002/2014PA002657

Key Points:
- Deep SW Atlantic was unlikely source of light carbon to atmosphere during HS1
- Mid-depth isotopic anomalies due to change in northern component water
- Northern component water had robust influence in South Atlantic during HS1

Correspondence to:
D. C. Lund,
david.lund@uconn.edu

Citation:
Lund, D. C., A. C. Tessin, J. L. Hoffman, and A. Schmittner (2015), Southwest Atlantic water mass evolution during the last deglaciation, *Paleoceanography*, *30*, 477–494, doi:10.1002/2014PA002657.

Received 8 APR 2014
Accepted 6 MAR 2015
Accepted article online 13 MAR 2015
Published online 6 MAY 2015

Southwest Atlantic water mass evolution during the last deglaciation

D. C. Lund[1], A. C. Tessin[2], J. L. Hoffman[2], and A. Schmittner[3]

[1]Department of Marine Sciences, University of Connecticut, Groton, Connecticut, USA, [2]Department of Earth and Environmental Sciences, University of Michigan, Ann Arbor, Michigan, USA, [3]College of Earth, Ocean, and Atmospheric Sciences, Oregon State University, Corvallis, Oregon, USA

Abstract The rise in atmospheric CO_2 during Heinrich Stadial 1 (HS1; 14.5–17.5 kyr B.P.) may have been driven by the release of carbon from the abyssal ocean. Model simulations suggest that wind-driven upwelling in the Southern Ocean can liberate ^{13}C-depleted carbon from the abyss, causing atmospheric CO_2 to increase and the δ^{13}C of CO_2 to decrease. One prediction of the Southern Ocean hypothesis is that water mass tracers in the deep South Atlantic should register a circulation response early in the deglaciation. Here we test this idea using a depth transect of 12 cores from the Brazil Margin. We show that records below 2300 m remained ^{13}C-depleted until 15 kyr B.P. or later, indicating that the abyssal South Atlantic was an unlikely source of light carbon to the atmosphere during HS1. Benthic δ^{18}O results are consistent with abyssal South Atlantic isolation until 15 kyr B.P., in contrast to shallower sites. The depth dependent timing of the δ^{18}O signal suggests that correcting δ^{18}O for ice volume is problematic on glacial terminations. New data from 2700 to 3000 m show that the deep SW Atlantic was isotopically distinct from the abyss during HS1. As a result, we find that mid-depth δ^{13}C minima were most likely driven by an abrupt drop in δ^{13}C of northern component water. Low δ^{13}C at the Brazil Margin also coincided with an ~80‰ decrease in Δ^{14}C. Our results are consistent with a weakening of the Atlantic meridional overturning circulation and point toward a northern hemisphere trigger for the initial rise in atmospheric CO_2 during HS1.

1. Introduction

The Last Glacial Maximum (LGM; ~20 kyr B.P.) was characterized by several major changes in the Earth's mean climate state, including the presence of massive continental ice sheets in North America and Eurasia [*Clark et al.*, 2009], an ~120 m lowering of global sea level [*Cutler et al.*, 2003], a 30% decrease in atmospheric CO_2 [*Monnin et al.*, 2001], and surface [*Shakun et al.*, 2012] and deep ocean temperatures several degrees colder than today [*Adkins et al.*, 2002]. Lower atmospheric CO_2 levels are thought to have been driven by sequestration of respired carbon in the abyssal ocean [*Broecker*, 1982; *Sigman and Boyle*, 2000]. Low benthic foraminiferal δ^{13}C values in the Atlantic [*Duplessy et al.*, 1988; *Curry and Oppo*, 2005], Indian [*Kallel et al.*, 1988], and Pacific Oceans [*Herguera et al.*, 2010] support the notion that ^{13}C-depleted carbon accumulated in the abyss.

Enhanced upwelling in the Southern Ocean and outgassing of carbon may have caused atmospheric CO_2 to rise during the last deglaciation [*Anderson et al.*, 2009]. Consistent with this idea, the initial 30 ppmv increase in atmospheric CO_2 from ~17.5 to 16 kyr B.P. coincided with a decrease in the δ^{13}C of CO_2 of 0.3‰ [*Monnin et al.*, 2004; *Schmitt et al.*, 2012; *Veres et al.*, 2012]. If the abyssal ocean was the source of light carbon, then benthic δ^{13}C and δ^{18}O records should record a change in the abyssal circulation at approximately the same time that atmospheric and surface ocean δ^{13}C decreased. The primary objective of this paper is to evaluate whether data from the southwest Atlantic support an abyssal ocean source for the initial rise in atmospheric CO_2. Although the abyssal southwest Atlantic clearly changed from ^{13}C-depleted to relatively ^{13}C-enriched values at some point during the deglaciation [*Curry and Oppo*, 2005], the precise timing of the shift has remained poorly constrained. Here we evaluate the timing using a depth transect of 12 cores from the Brazil Margin spanning 400 m to 4000 m water depth (Figure 1). Each core is placed into a common chronologic framework to minimize relative differences in timing, and the resulting time series are cross checked using records at adjacent water depths. Vertical profiles of δ^{13}C and δ^{18}O at discrete time steps are then used to evaluate the timing of circulation changes in different parts of the water column.

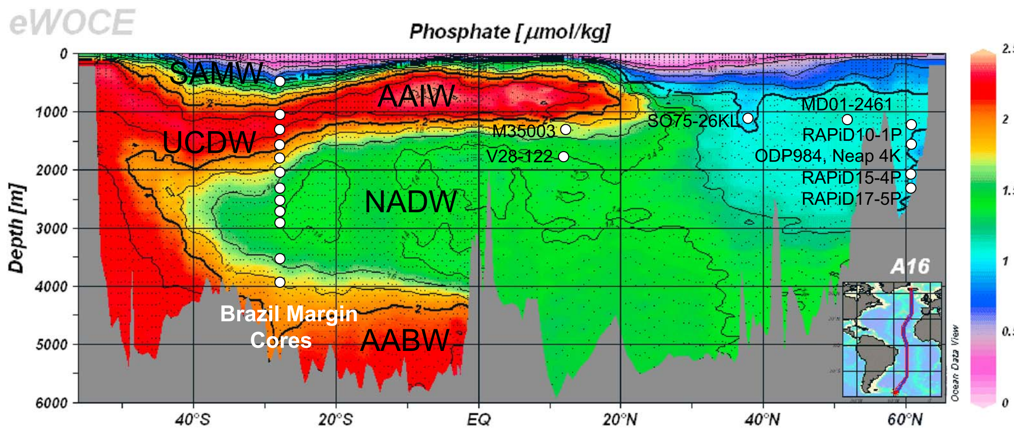

Figure 1. Locations of the 12 cores used in this paper (Table 1) superimposed on the phosphate concentration of the World Ocean Circulation Experiment A16 section in the Atlantic Ocean [*Schlitzer*, 2000]. The Brazil Margin cores at 27°S span Antarctic Intermediate Water (AAIW), Upper Circumpolar Deep Water (UCDW), and North Atlantic Deep Water (NADW). Also shown are the approximate core locations for NEAP 4 K [*Rickaby and Elderfield*, 2005], ODP984 [*Praetorius et al.*, 2008], RAPiD 10-1P, RAPiD 15-4P and RAPiD 17-5P [*Thornalley et al.*, 2010], SO75-26KL [*Zahn et al.*, 1997], M35003 [*Zahn and Stuber*, 2002], V28-122 [*Yu et al.*, 2010], and MD01-2461 [*Peck et al.*, 2006].

A secondary objective is to evaluate the source of negative carbon isotope excursions at the Brazil Margin. Carbon isotope minima were ubiquitous in the surface and mid-depth Atlantic during the deglaciation [*Oppo and Fairbanks*, 1989; *Curry et al.*, 1988; *Slowey and Curry*, 1995; *Peck et al.*, 2006; *Thornalley et al.*, 2010]. The largest anomalies occurred in the mid-depth North Atlantic, with $\delta^{13}C$ decreasing up to 1‰ at multiple locations [*Zahn et al.*, 1997; *Zahn and Stuber*, 2002; *Rickaby and Elderfield*, 2005; *Peck et al.*, 2006; *Praetorius et al.*, 2008; *Thornalley et al.*, 2010; *Oppo et al.*, 2015]. The source of the $\delta^{13}C$ minima remains controversial, and several mechanisms have been proposed, including regional brine formation [*Dokken and Jansen*, 1999; *Waelbroeck et al.*, 2011], greater incursion of southern source intermediate water [*Rickaby and Elderfield*, 2005], and weakening of the Atlantic meridional overturning circulation [*Zahn et al.*, 1997]. *Tessin and Lund* [2013] argued that the mid-depth anomalies at the Brazil Margin could not be easily explained by the incursion of southern component water (SCW) or by mixing between abyssal SCW and northern component water (NCW). Here we present new results from 2700 m and 2900 m water depth that better define SCW properties during the deglaciation. Using these new data, we re-evaluate potential drivers of the mid-depth anomalies.

2. Methods

2.1. Stable Isotopic Records

The cores developed for this study were raised from the Brazil Margin during cruise KNR159-5 (Table 1). The cores include 14GGC (440 m water depth), 90GGC (1105 m), 63GGC (2732 m), and 20JPC (2951 m). Stable isotope results for 14GGC and 90GGC were presented in *Curry and Oppo* [2005]. For 63GGC and 20JPC, samples were taken at 4 to 5 cm intervals, freeze-dried, and washed through a 63 μm sieve. Each sample was picked for *Cibicidoides wuellerstorfi* (>250 μm size fraction), and individual tests were analyzed for $\delta^{18}O$ and $\delta^{13}C$ using standard procedures [*Hoffman and Lund*, 2012]. Samples from 20JPC were also picked for *Globigerinoides ruber* (>250 μm size fraction) to evaluate the stratigraphic integrity of the core; 6–7 tests were used for each isotopic analysis. Both benthic and planktonic samples were run on a triple-collector gas source mass spectrometer coupled to a Finnigan Kiel automated preparation device at the Stable Isotope Laboratory at the University of Michigan. Data were converted to Vienna Peedee belemnite using NBS 19 ($n = 27$, $\delta^{13}C = 1.94 \pm 0.04$, $\delta^{18}O = -2.21 \pm 0.06$‰) and NBS 18 ($n = 20$, $\delta^{13}C = -5.02 \pm 0.04$, $\delta^{18}O = -22.99 \pm 0.08$‰). Atlantis II standards were analyzed to constrain benthic $\delta^{18}O$ results at the "heavy" end of the oxygen isotopic scale; the results ($n = 23$, $\delta^{13}C = 0.92 \pm 0.06$, $\delta^{18}O = 3.44 \pm 0.05$‰) are consistent with established values for Atlantis II [*Ostermann and Curry*, 2000].

2.2. Age Models and Benthic $\Delta^{14}C$

The age models for the Brazil Margin cores are based on radiocarbon dates of the planktonic foraminifer *G. ruber* (>250 μm size fraction). The weights of *G. ruber* samples used for ^{14}C analysis ranged between 1 and

Table 1. Summary of Stable Isotope and Age Model Results Synthesized in This Paper, Including Data From *Curry and Oppo* [2005] (CO2005), *Sortor and Lund* [2011] (SL2011), *Hoffman and Lund* [2012] (HL2012), and *Tessin and Lund* [2013] (TL2013)[a]

Depth (m)	Core	Age Model	Stable Isotopes	Extrapolated values (kyr B.P.)
440	14GGC	this paper	CO2005	not available (na)
1105	90GGC	this paper	CO2005	20–23
1296	36GGC	SL2011	CO2005	na
1627	17JPC	TL2013	TL2013	23
1829	78GGC	TL2013	TL2013	21–23
2082	33GGC	TL2013	TL2013	1
2296	42JPC	HL2012	CO2005	na
2500	30GGC	TL2013	TL2013	1–2
2732	63GGC	this paper	this paper	1–2
2951	20JPC	this paper	this paper	1–2
3589	125GGC	HL2012	HL2012	1–4, 23
3924	22GGC	HL2012	HL2012	1–6

[a]Time intervals that required extrapolation of existing stable isotope records are noted in the last column.

5 mg. In cases where the total mass of *G. ruber* was less than 1 mg, the samples were supplemented with *G. sacculifer* (>250 μm). Samples were prepared for ^{14}C analysis following standard procedures at the Keck Carbon Cycle Accelerated Mass Spectrometer Laboratory at the University of California Irvine. We used a Δ*R* of zero years to constrain surface water reservoir ages. The modern surface water reservoir at 27°S on the Brazil Margin is 407 ± 59 years, equivalent to a Δ*R* of 7 ± 59 (*n* = 12) [*Angulo et al*., 2005]. We used a Δ*R* error of ±200 years (1σ) to account for unknown changes in reservoir age through time. Calendar ages for 14GGC, 90GGC, 63GGC, and 20JPC were calibrated using *Calib v.7.0* (http://calib.qub.ac.uk/calib/calib.html) (Table 2). To ensure consistency amongst the Brazil Margin records, all published radiocarbon ages for the cores were re-calibrated using *Calib v.7.0*.

Benthic radiocarbon analyses were performed on 21 samples from core 78GGC. In each case, the analyses were based on 5–10 mg of *Uvigerina* spp. from the >250 μm size fraction (Table 3). Previous work at the Brazil Margin suggests that ^{14}C-dates based on *Cibicidoides* spp. and *Uvigerina* spp. from the same samples yield similar ages [*Sortor and Lund*, 2011]. Following the method outlined in *Lund et al*. [2011b], our estimates of deepwater $\Delta^{14}C$ were made by age correcting the benthic ^{14}C results with calendar ages determined using planktonic foraminifera from the same sample. The resulting error bars for each benthic $\Delta^{14}C$ estimate represent the compounded analytical and calendar age uncertainty, determined using a Monte Carlo approach.

2.3. Vertical Profiles

Once each core was placed into a common chronologic framework, the records were interpolated at 1 kyr intervals from 1 to 23 kyr B.P. In order to preserve the timing of isotopic variability in each core, no smoothing function was applied. Although this yields somewhat noisier results for the low-resolution Holocene portion of the records, it facilitates comparison with other paleoclimate archives. In some cases, the Brazil Margin time series did not span the entire 1 to 23 kyr B.P. time interval. In these instances, the missing values were determined by extrapolation of the nearest results in the same core (Table 1). The extrapolated values represent <10% of the total data points used in the vertical profiles. These data have little influence on the key results presented here because the points are exclusively from the LGM and late Holocene intervals. As shown below, both are periods of relatively stable water mass conditions at the Brazil Margin.

2.4. Northern Component Water Time Series

Determining whether the Brazil Margin stable isotopic records reflect the influence of northern component water requires the creation of a representative time series from the North Atlantic. We used three cores to create a stacked record for the subpolar North Atlantic, including ODP984, NEAP4K, and RAPiD-10-1P (Table 4). The two other cores listed in Table 4 have benthic $\delta^{13}C$ histories very similar to the subpolar North Atlantic sites but their $\delta^{18}O$ values are generally lower given their lower latitude locations. As a result, they were not included in the stacked record. Note that all of the cores are from the upper portion of the water column (1150–1650 m) to minimize influence of intermediate and mode waters and to avoid the large vertical $\delta^{18}O$ gradient during HS1. Cores from a similar depth range are used by *Oppo et al*. [2015] to constrain

10.1002/2014PA002657

Table 2. Planktonic Radiocarbon Results for Cores Presented in This Paper[a]

Core	Depth (cm)	^{14}C age (years)	Error (years)	Calendar Age (yr B.P.)	Error (years)	Notes	University of California-Irvine Accelerator Mass Spectrometry (UCIAMS) No.
KNR159-5-14GGC	3	1,605	15	1,138	203		94943
	25	3,185	15	2,990	236		94944
	57	5,965	20	6,404	221		94945
	73	7,170	20	7,651	186		94946
	89	9,210	20	9,955	262		94947
	97	11,575	40	13,045	202		94948
	114	14,160	40	16,630	307		94950
	122	13,815	40	16,125	297		94951
	118	13,987.5	40	16,378	427	average	n/a
	170	16,060	230	18,939	344		94952
KNR159-5-90GGC	30.5	4,790	20	5,064	248		92724
	40.5	6,065	20	6,497	219		92725
	50.5	8,000	25	8,490	246		92726
	60.5	10,640	25	12,005	385		92727
	70.5	12,080	30	13,546	205		92728
	80.5	11,620	25	13,087	201		92729
	75.5	11,850	39	13,317	287	average	n/a
	90.5	12,630	30	14,252	361		92730
	100.5	13,500	75	15,668	316		OS-27754
	104.5	12,180	30	13,635	211	reversal	92731
	110.5	11,530	30	12,998	199	reversal	92732
	120.5	11,210	30	12,736	206	reversal	92733
	130.5	10,805	30	12,263	302	reversal	92734
	140.5	9,395	25	10,227	272	reversal	92735
	144.5	12,450	50	13,921	285	reversal	OS-34253
	150.5	11,665	25	13,125	202	reversal	92736
	200.5	16,700	95	19,689	281		OS-27755
KNR159-5-63GGC	6.5	3,145	15	2,964	237		109707
	14	8,310	20	8,844	262		154411
	18.5	11,590	40	13,060	202		142506
	21.5	12,150	40	13,608	210		142507
	24.5	11,580	100	13,047	217	reversal	109708
	30.5	14,930	90	17,693	267		154412
	35	15,840	140	18,677	259		154413
	42.5	11,665	40	12,810	520	reversal	109709
	48.5	17,610	60	20,758	273		142508
	60.5	17,600	80	20,748	281		109710
	54.5	17,605	100	20,753	391	average	n/a
	78.5	19,890	260	23,454	395		109711
	96.5	24,430	170	28,077	257		109712
KNR159-5-20JPC	5.5	2,935	20	2,670	254		92737
	10.5	4,155	25	4,224	273		92738
	25.5	7,515	25	7,974	205		92739
	35.5	10,640	25	12,005	385		92740
	45.5	9,385	30	10,215	275	reversal	92741
	60.5	3,585	20	3,481	255	reversal	92742
	70.5	9,180	70	9,926	269	reversal	92743
	71.5	5,540	25	5,941	222	reversal	94722
	80.5	10,840	320	12,171	518	reversal	92744
	90.5	4,805	45	5,071	253	reversal	92745
	95.5	4,245	35	4,345	280	reversal	92746
	105.5	7,230	100	7,713	207	reversal	92747
	115.5	12,780	170	14,520	440	reversal	92748
	120.5	14,340	250	16,891	458		92749
	135.5	16,270	370	19,175	471		92804

Table 2. (continued)

Core	Depth (cm)	^{14}C age (years)	Error (years)	Calendar Age (yr B.P.)	Error (years)	Notes	University of California-Irvine Accelerator Mass Spectrometry (UCIAMS) No.
KNR159-5-20JPC	145.5	13,600	300	15,798	415	reversal	92805
	170.5	17,270	80	20,335	262		92806
	174	17,740	160	20,933	343		94723

[a]In instances where nearby planktonic samples had calendar ages within ±1 standard deviation, the samples were averaged to produce a mean age. All of the dates are based on *G. ruber*, and all were run at UC Irvine with the exception of three samples for KNR159-5-90GGC, which were run at Woods Hole Oceanographic Institution (WHOI) National Ocean Sciences Accelerator Mass Spectrometry (100.5 cm, 144.5 cm, and 200.5 cm). These three dates were provided by Delia Oppo. n/a, not applicable.

NCW during the deglaciation. In the North Atlantic, $\delta^{18}O$ values below 2000 m are ~1‰ higher than those from 1150 to 1650 m (see Figure 9 in *Tessin and Lund* [2013]). In the South Atlantic, there is also clear stepwise increase in $\delta^{18}O$ between 2000 and 2500 m during HS1 (see Results section below).

Age models for the North Atlantic records were developed using a combination of ^{14}C ages and tie points. Radiocarbon ages for ODP984 [*Praetorius et al.*, 2008] were re-calibrated using *Calib v.7.0* to ensure consistency with the Brazil Margin results. For the deglaciation (20–10 kyr B.P.), we used the regionally averaged high-latitude North Atlantic surface water reservoir ages presented in Table S4 of the supporting information for *Stern and Lisiecki* [2013], which reach a maximum of 1260 years during HS1 (i.e., a ΔR of 860 years). These reservoir ages yield calendar ages that are approximately 1 kyr younger, meaning that the abrupt shift in $\delta^{13}C$ and $\delta^{18}O$ occurs at ~18 kyr B.P. rather than ~19 kyr B.P., in good agreement with core M35003 from the subtropical North Atlantic. For the LGM and Holocene sections of ODP984, we used a ΔR of 0 ± 200 years (1σ) to account for the subtler reservoir age variability estimated for these time intervals [*Stern and Lisiecki*, 2013]. Following *Oppo et al.* [2015], we also added a tie point based on correlation of the ODP984 % *Neogloboquadrina pachyderma (s)* record to GISPII $\delta^{18}O$ at 14.5 kyr B.P.

Given its lack of radiocarbon ages, the age model for NEAP4K is based on correlation of its benthic $\delta^{13}C$ time series to the well-dated $\delta^{13}C$ record of M35003 in the subtropical North Atlantic. (Ages for M35003 were

Table 3. Benthic Radiocarbon Results for Core KNR-159-5-78GGC[a]

Depth (cm)	Genera	^{14}C age (years)	Error (years)	Fraction modern	Error	B.P. Age (years)	$\Delta^{14}C$ (‰)	Notes	UCIAMS No.
1	*Uvig.*	2,305	35	0.7506	0.0029	1,070	−173		109736
9	*Uvig.*	6,260	40	0.4587	0.0021	450	−28		109737
13	*Uvig.*	9,040	70	0.3247	0.0025	1,510	−147		109738
17	*Uvig.*	10,535	45	0.2694	0.0014	1,735	−153		109739
25	*Uvig.*	12,055	40	0.2230	0.0010	1,665	−106		109740
33	*Uvig.*	13,295	45	0.1911	0.0010	820	30		109741
37	*Uvig.*	13,715	40	0.1813	0.0009	1,030	19		109742
45	*Uvig.*	14,490	70	0.1647	0.0014	1,055	100		109743
49	*Uvig.*	14,730	60	0.1598	0.0010	945	164		109744
57	*Uvig.*	15,105	50	0.1525	0.0009	1,000	166		109745
61	*Uvig.*	15,050	50	0.1536	0.0009	985	168		109746
59		15,078	71	0.1531	0.0013	993	167	average	
89	*Uvig.*	15,790	45	0.1401	0.0007	830	193		109747
97	*Uvig.*	15,840	40	0.1392	0.0007	800	195		109748
105	*Uvig.*	15,810	50	0.1397	0.0008	450	271		109749
113	*Uvig.*	16,295	50	0.1316	0.0008	570	254		109750
117	*Uvig.*	16,520	60	0.1278	0.0009	800	192		109751
115		16,408	78	0.1297	0.0012	685	222	average	
125	*Uvig.*	16,900	60	0.1220	0.0008	740	212		109752
137	*Uvig.*	17,250	70	0.1168	0.0009	550	225		109753
145	*Uvig.*	17,440	60	0.1141	0.0008			reversal	109754
153	*Uvig.*	17,720	80	0.1101	0.0010	730	193		109755
165	*Uvig.*	17,590	60	0.1119	0.0008			reversal	109756

[a]Results at 145 cm and 165 cm are planktonic ^{14}C age reversals, most likely due to bioturbation. In instances where nearby planktonic samples had radiocarbon ages within $\pm1\sigma$, the samples were averaged (57 cm and 61 cm; 113 and 117 cm).

Table 4. Locations and Water Depths of Published High-Resolution North Atlantic Records Used in This Paper

Core	Latitude (°N)	Longitude (°W)	Water Depth (m)	Reference
ODP984	61°25′	24°04′	1648	*Praetorius et al.* [2008]
NEAP 4 K	61°30′	24°10′	1627	*Rickaby and Elderfield* [2005]
RAPiD-10-1P	62°59′	17°35′	1237	*Thornalley et al.* [2010]
M35003	12°5′	61°15′	1299	*Zahn and Stuber* [2002]
MD01-2461	51°45′	12°55′	1153	*Peck et al.* [2006]

re-calibrated using *Calib v.7.0* and an assumed Δ*R* of 0 ± 200 years.) This region is less likely to experience large changes in surface water reservoir age than the high-latitude North Atlantic. The M35003 benthic $\delta^{13}C$ record bears a strong resemblance to ODP984, NEAP 4 K, and mid-depth time series from the Brazil Margin.

The age model for RAPiD-10-1P is well constrained from 1 to 15 kyr B.P. based on a combination of radiocarbon ages, ash layers, and correlation of its % *N. pachyderma (s)* record to NGRIP $\delta^{18}O$ [*Thornalley et al.*, 2010]. Prior to 15 kyr B.P., however, the age model lacks solid age constraints. We therefore assigned an age of 18 kyr B.P. to the beginning of the 1‰ decrease in benthic $\delta^{13}C$ at 270 cm so that its $\delta^{13}C$ record is consistent with the ODP984 and M35003 time series.

3. Results

3.1. Brazil Margin Age Models

The age models for Brazil Margin cores 14GGC, 90GGC, and 63GGC are shown in Figure 2. Calendar ages for 14GGC display a monotonic increase with depth with the exception of a small reversal at 122 cm. Given that the ages at 114 cm and 122 cm overlap at one sigma, the results were averaged to create a single age control point. The age model for 90GGC is less well behaved and shows a broad interval of unusually young ages from 105 cm to 150 cm. Core 63GGC also displays reversals at 24.5 cm and 42.5 cm. Age reversals of similar magnitude exist in other Brazil Margin cores. Detailed analysis of radiocarbon ages and individual benthic foraminifera suggests that the reversals are the result of deep burrowing that carries young material down-section [*Sortor and Lund*, 2011; *Tessin and Lund*, 2013]. Here we assume that a similar phenomena occurred in 90GGC and 63GGC and discard the anomalously young ages. The resulting age model yields $\delta^{18}O$ and $\delta^{13}C$ time series consistent with results from shallower and deeper in the water column.

The age model for core 20JPC displays age reversals of several thousand years (Figure 3, top). The reversals are focused in the 50 to 100 cm interval with an additional smaller reversal at 145 cm. Given the large amplitude

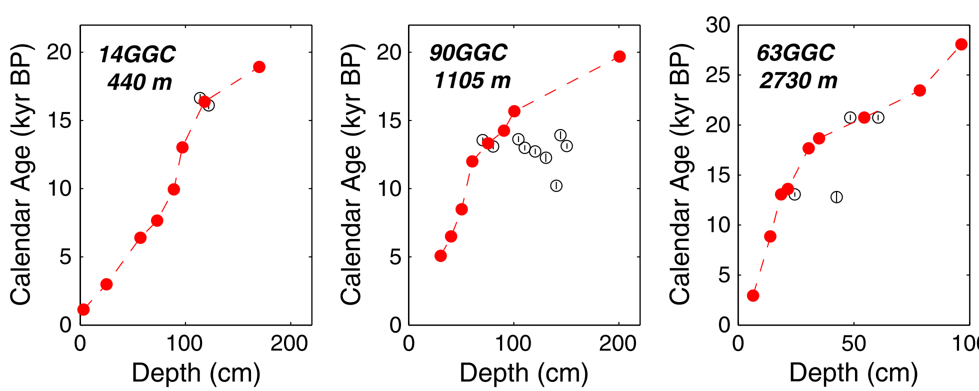

Figure 2. Calendar ages (red circles) and age models (dashed lines) for cores KNR159-5-14GGC, KNR159-5-90GGC, and KNR159-5-63GGC based on *G. ruber* (>250 μm). The error bars for each calendar age represent the ±1σ uncertainty. In most cases, the error bar is smaller than the symbol. Age reversals not included in each age model are shown as black circles. In the case of 14GGC, the two ages near 120 cm were averaged to create one control point. Cores 90GGC and to a lesser extent 63GGC have ages out of stratigraphic order. A similar phenomenon occurs in other Brazil Margin cores and is related to deep burrowing [*Sortor and Lund*, 2011; *Hoffman and Lund*, 2012] and the variable abundance of planktonic and benthic foraminifera (see Figure 3). Note that the benthic stable isotopic time series for cores 14GGC, 90GGC, and 63GGC lack obvious evidence of bioturbation from up section (Figure 4).

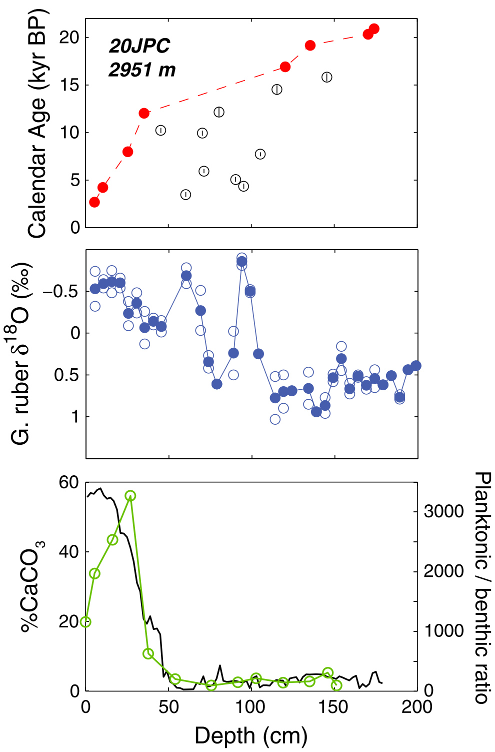

Figure 3. (top) Calendar ages (red circles) and age model (dashed line) for core KNR159-5-20JPC based on the planktonic foraminifer *G. ruber* (>250 μm). The error bars for each calendar age represent the ±1σ uncertainty. Reversals not included in the age model are shown as black symbols. (middle) *G. ruber* $\delta^{18}O$ (>250 μm) for core KNR159-5-20JPC, including individual analysis based on 6–7 individuals (open symbols) and the average value at each stratigraphic level (solid symbols). The ^{14}C ages and the $\delta^{18}O$ results indicate the presence of disturbed sediment from 50 to 110 cm. Both proxies suggest the material originated from the upper 20 cm of the stratigraphy. (bottom) The %$CaCO_3$ (black) and the ratio of planktonic to benthic foraminiferal shells (green) in 20JPC.

of the features, we performed stable isotope analyses on *G. ruber* (>250 μm) from the same samples to determine if burrowing was responsible. The *G. ruber* $\delta^{18}O$ results show clear evidence for disturbance of the planktonic stratigraphy; negative $\delta^{18}O$ excursions centered at 60 cm and 95 cm align with the age reversals (Figure 3, middle). Both the age reversals and low $\delta^{18}O$ values can be explained by burrowing of material from the Holocene portion of the record.

The Holocene section of 20JPC is characterized by high %$CaCO_3$ and a high ratio of planktonic to benthic foraminiferal shells (Figure 3, bottom). The planktonic/benthic ratio is 10–30 times greater during the Holocene than deglaciation. As a result, downward burrowing of Holocene material will have a greater influence on planktonic ^{14}C ages and $\delta^{18}O$ than on the benthic stable isotopic records. We therefore exclude anomalously young ages from the age model for 20JPC. As shown below, there is no evidence of Holocene benthic foraminifera in the 50–100 cm depth range, most likely due to the low planktonic/benthic ratio in this part of the stratigraphy.

3.2. Stable Isotope Time Series

The benthic stable isotopic records for 14GGC, 90GGC, 63GGC, and 20JPC are shown in Figure 4. Overall, $\delta^{18}O$ follows the expected pattern during the deglaciation, decreasing by 1.8‰ at the shallower sites and 2.0‰ at the deeper sites. The larger glacial-interglacial $\delta^{18}O$ difference at the deeper sites is consistent with the depth-dependent pattern in $\delta^{18}O$ observed in other Brazil Margin records [*Curry and Oppo*, 2005; *Lund et al.*, 2011a]. At both shallow sites, $\delta^{18}O$ decreased beginning 17–18 kyr B.P., whereas at the deeper sites, $\delta^{18}O$ decreased at starting at ~15 kyr B.P. (Figure 4). The age reversal intervals in each core (grey bars) do not contain benthics from the Holocene portion of the stratigraphy. If downward burrowing of benthics from the Holocene did occur, it would cause the deglacial shift in $\delta^{18}O$ to occur earlier rather than later. At 2500 m and 3589 m water depth, the primary shift in benthic $\delta^{18}O$ also occurred after 15 kyr B.P. [*Tessin and Lund*, 2013; *Hoffman and Lund*, 2012]. The overall agreement between four records spanning 2500 m to 3600 m water depth and the lack of evidence for bioturbation of benthics indicates that the cores yield a reliable picture of $\delta^{18}O$ variability during the deglaciation.

Similar to $\delta^{18}O$, the deglacial evolution of benthic $\delta^{13}C$ varies with water depth. At 440 m, the 0.4‰ increase in benthic $\delta^{13}C$ from the LGM to Holocene is interrupted by a 0.3‰ negative excursion beginning at ~16 kyr B.P. The amplitude of the $\delta^{13}C$ anomaly is approximately half that at mid-depths, and it occurred >1 kyr later [*Tessin and Lund*, 2013]. In contrast, $\delta^{13}C$ at 1105 m increased monotonically during the deglaciation from 0.4‰ at the LGM to 1.3‰ in the late Holocene, a total change of 0.9‰. This is similar to but larger than the 0.5‰ deglacial shift that occurred at 1268 m water depth [*Curry and Oppo*, 2005]. At both 2732 m and 2951 m, $\delta^{13}C$ decreased slightly from 21 to 15 kyr B.P. and then increased. The $\delta^{13}C$ time series at 2500 m [*Tessin and Lund*, 2013] and 3589 m [*Hoffman and Lund*, 2012] show a similar pattern.

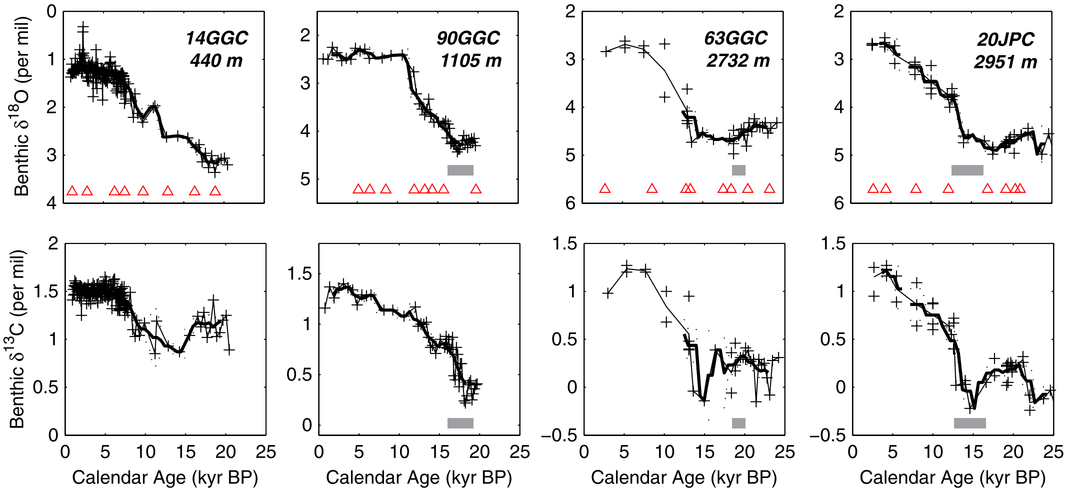

Figure 4. (top row) *C. wuellerstorfi* $\delta^{18}O$ time series for the Brazil Margin. Each panel includes $\delta^{18}O$ results for individual foraminifera (plus sign), the average value at each stratigraphic level (thin line), the 2000 year running mean (thick line), and the standard error on the running mean (dashed lines). The red triangles denote calendar ages for each core. Note that each *y* axis spans 4‰. (bottom row) Same as above except showing *C. wuellerstorfi* $\delta^{13}C$. Each *y* axis spans 2‰. The grey bars indicate the approximate interval of disturbed sediment as indicated by the age models (Figures 2 and 3). Unlike the age models, the benthic stable isotopic time series lack evidence of deep burrowing from up-section. Both 63GGC and 20JPC show the primary deglacial increase in $\delta^{13}C$ and decrease in $\delta^{18}O$ occurs after 15 kyr BP.

3.3. Benthic $\Delta^{14}C$ Time Series

Benthic $\Delta^{14}C$ results for core 78GGC (1820 m water depth) are displayed in Figure 5. In the top panel, reconstructed $\Delta^{14}C$ values are plotted along with the INTCAL13 atmospheric $\Delta^{14}C$ curve and an estimate of $\Delta^{14}C$ at 1820 m water depth assuming a ^{14}C age of 850 years [*Stuiver and Ostlund*, 1980]. Estimates of $\Delta\Delta^{14}C$ (reconstructed benthic $\Delta^{14}C$—atmospheric $\Delta^{14}C$) show that ^{14}C at 1800 m was generally depleted during the deglaciation, reaching values as low as −260‰ (Figure 5, middle). This is similar to the −250‰ difference between deep northeast Pacific and atmospheric $\Delta^{14}C$ today [*Key et al*., 2004]. The LGM to HS1 transition is marked by a shift in $\Delta\Delta^{14}C$ of ~70‰. The overall pattern in 78GGC $\Delta\Delta^{14}C$ is similar to the benthic $\delta^{13}C$ record, with each time series showing a broad deglacial minimum. The largest $\Delta\Delta^{14}C$ anomaly appears to have occurred late in the deglaciation, however, whereas the maximum $\delta^{13}C$ anomaly occurred during HS1.

3.4. Northern Component Water

The stacked $\delta^{18}O$ record for the subpolar North Atlantic was generally stable during the LGM and then decreased abruptly beginning at ~18 kyr B.P. (Figure 6). The $\delta^{18}O$ then stabilized before decreasing again at ~12 kyr B.P., reaching stable Holocene values by ~7 kyr B.P. The records at 12°N and 52°N generally have more depleted ^{18}O values due to their lower latitude locations. Benthic $\delta^{13}C$ variability is similar among all of the North Atlantic cores, although the data at 12°N are generally more depleted, presumably due to mixing with southern source water. The stacked $\delta^{13}C$ record shows a 0.8‰ decrease at the beginning of HS1. Note that all of the North Atlantic records converge on a similar $\delta^{13}C$ value by 17 kyr B.P. Averaging the HS1 intervals in the five cores yields a $\delta^{13}C$ of 0.72 ± 0.12‰ (1σ) and $\delta^{18}O$ of 3.12 ± 0.14‰ (1σ). If we instead define HS1 as the interval with lowest $\delta^{13}C$ in the five cores, the mean $\delta^{13}C$ is 0.61 ± 0.04‰ (1σ) and the mean $\delta^{18}O$ is 3.04 ± 0.24‰ (1σ). *Oppo et al*. [2015] used a different combination of cores from the subpolar North Atlantic and found similar HS1 $\delta^{13}C$ and $\delta^{18}O$ values (0.6‰ and 3.2‰, respectively). Although $\delta^{13}C$ and $\delta^{18}O$ vary somewhat depending on location, the differences are small relative to the large isotopic shift during HS1.

3.5. Brazil Margin Vertical Profiles

Vertical profiles of $\delta^{13}C$ and $\delta^{18}O$ for the Brazil Margin are shown in Figure 7. During the LGM, the influence of Glacial Antarctic Bottom Water (GAABW) is apparent in the abyssal portion of the $\delta^{13}C$ profile, as is Glacial North

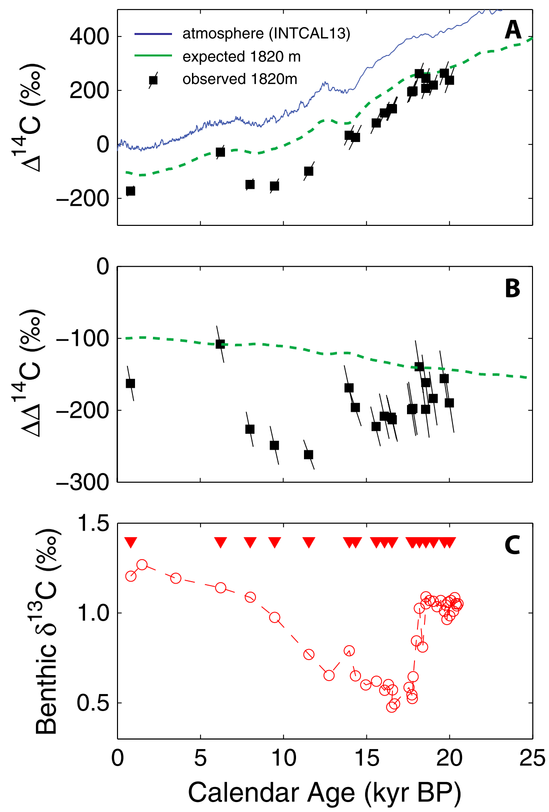

Figure 5. Benthic radiocarbon results for core KNR159-5-78GGC at 1820 m water depth on the Brazil Margin. (a) Benthic $\Delta^{14}C$ estimates (black squares). The INTCAL13 atmospheric $\Delta^{14}C$ record (blue line) [*Reimer et al.*, 2013] and the expected $\Delta^{14}C$ at 1820 m for the southwest Atlantic (green dashed line) are also shown. The expected curve was determined using INTCAL13 atmospheric $\Delta^{14}C$ and the modern ^{14}C age at 1820 m of 850 years [*Stuiver and Ostlund*, 1980]. (b) Difference between the reconstructed $\Delta^{14}C$ for 78GGC and atmospheric $\Delta^{14}C$ ($\Delta\Delta^{14}C$). (c) Benthic $\delta^{13}C$ time series for 78GGC (red circles). The calendar calibrated ages (red triangles) are also shown.

Atlantic Intermediate Water (GNAIW) from 1500 m to 2000 m, and Glacial Antarctic Intermediate Water (GAAIW) from ~800 m to 1200 m. During HS1 (16–17 kyr B.P.), $\delta^{13}C$ decreased at mid-depths (1300–2500 m) but remained essentially unchanged below 2500 m. Only after 15 kyr B.P. did $\delta^{13}C$ increase in the deeper portion of the water column, lagging the negative carbon isotopic excursion at mid-depths by ~2 kyr (Figure 8). By the early Holocene (7–9 kyr B.P.), a quasi-modern $\delta^{13}C$ profile began to emerge, with ^{13}C-depleted water in the abyss, ^{13}C-enriched water from ~2000 m to 3000 m, and ^{13}C-depleted water from ~1300 m to 1800 m (Figure 7). In the modern southwest Atlantic, these depths correspond to AABW, North Atlantic Deep Water (NADW), and upper Circumpolar Deep Water (UCDW), respectively. A stable Holocene $\delta^{13}C$ profile was established by approximately 5 kyr B.P.

Benthic $\delta^{18}O$ at the Brazil Margin either remained constant or decreased during the deglaciation. Maximum $\delta^{18}O$ values in the abyss during the LGM reflect the presence of GAABW, while progressively lower $\delta^{18}O$ at shallower depths reflect the influence of GNAIW [*Curry and Oppo*, 2005; *Hoffman and Lund*, 2012]. During HS1, $\delta^{18}O$ values decreased above 2200 m but remained essentially constant between 2500 m and 3500 m, creating a large vertical gradient in $\delta^{18}O$ from 2000 m to 2500 m. Benthic $\delta^{18}O$ also decreased at the deepest sites early in the deglaciation, implying that isotopically depleted and/or warmer water entered into the abyssal SW Atlantic from the south (Figure 8). Later in the deglaciation, high $\delta^{18}O$ centered at 3 km water depth was apparently eroded by mixing from above and below. The $\delta^{18}O$-delineated water mass boundary between 2000 m and 2500 m persisted throughout the deglaciation and into the early Holocene, however. By 7 kyr B.P., the "step" in $\delta^{18}O$ disappears, broadly consistent with the timing of sea level stabilization [*Cutler et al.*, 2003; *Thompson and Goldstein*, 2006]. It therefore appears that the primary driver of $\delta^{18}O$ stratification at the Brazil Margin was input of isotopically light water from melting of the Northern Hemisphere ice sheets. This inference will require verification with temperature estimates based on benthic foraminiferal Mg/Ca.

4. Discussion

4.1. Evolution of the Deep SW Atlantic

The primary aim of developing detailed isotopic records from the Brazil Margin was to create a series of discrete vertical profiles that could be used to infer water mass properties in the southwest Atlantic during Termination I. In particular, our goal was to test whether circulation tracers in the abyssal southwest Atlantic changed in step with the decline in atmospheric $\delta^{13}C$. Both the vertical profiles (Figure 7) and contoured benthic $\delta^{13}C$ anomalies (Figure 8) suggest that this was not the case. Benthic $\delta^{13}C$ in the abyssal SW Atlantic showed little change early in the deglaciation, with only the deepest site showing signs of a positive $\delta^{13}C$ shift by 16 kyr B.P. Prior to this time, $\delta^{13}C$ either decreased or remained stable at all depths

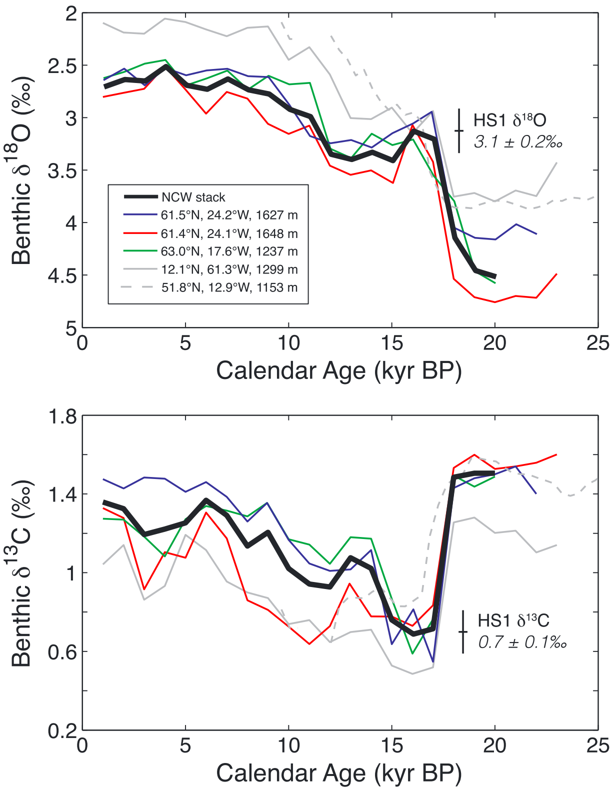

Figure 6. Benthic $\delta^{18}O$ and $\delta^{13}C$ time series from the North Atlantic spanning the LGM to present, including NEAP 4 K (blue) [*Rickaby and Elderfield*, 2005], ODP948 (red) [*Praetorius et al.*, 2008], RAPiD 10-1P (green) [*Thornalley et al.*, 2010], M35003 (grey) [*Zahn and Stuber*, 2002], and MD01-2461 (grey dashed) [*Peck et al.*, 2006]. Each record has been interpolated at 1 kyr intervals from 1 to 23 kyr B.P.. The three subpolar North Atlantic records were averaged to create representative $\delta^{18}O$ and $\delta^{13}C$ time series for northern component water (NCW). The remaining two records (in grey) were excluded due to their geographic location and generally lower $\delta^{18}O$ values. Mean HS1 $\delta^{18}O$ and $\delta^{13}C$ values were calculated using data from the 14.5–17.5 kyr B.P. interval from all five cores.

below 1500 m. The primary HS1 signal between 2500 m and 3000 m water depth was negative, due to downward propagation of the anomaly from mid-depths (Figure 8). From 2500 to 3500 m, the primary increase in $\delta^{13}C$ occurred after 15 kyr B.P., well after the initial decline in atmospheric $\delta^{13}C$ at 17 kyr B.P. [*Veres et al.*, 2012; *Parrenin et al.*, 2013]. Benthic $\delta^{18}O$ results are also consistent with isolation of the deep southwest Atlantic early in the deglaciation. Benthic $\delta^{18}O$ from 2500 m to 3600 m remained largely unchanged from the LGM until 16 kyr B.P. or later (Figure 8). This is also demonstrated in crossplots of the Brazil Margin data that show steady deep and abyssal stable isotopic values until at least 16 kyr B.P. (Figure 9, top). The primary shift in benthic $\delta^{18}O$ and $\delta^{13}C$ occurred from ~15 to 9 kyr B.P.

The timing of the primary $\delta^{13}C$ decrease at the deep Brazil Margin sites appears to be consistent with other abyssal ocean records. In the Atlantic sector of the Southern Ocean, benthic $\delta^{13}C$ at 3.8 km water depth decreased beginning at ~15 kyr B.P. [*Waelbroeck et al.*, 2011]. A reduction in the Southern Ocean vertical $\Delta^{14}C$ gradient, inferred to represent enhanced vertical mixing, also occurred at approximately 15 kyr B.P. [*Burke and Robinson*, 2012]. The available data therefore do not appear to support an abyssal South Atlantic contribution to the atmospheric $\delta^{13}C$ signal during HS1. If enhanced ventilation in another part of the deep ocean liberated ^{13}C-depleted carbon, the southwest Atlantic must have been insulated from the effect of the circulation change. This seems unlikely, however, given that records from 4.2 km in the Indian Ocean and 3.4 km in the Pacific also show an initial shift in $\delta^{13}C$ at ~15 kyr B.P. [*Yu et al.*, 2010]. Higher-resolution records from the deep northeast Pacific also support a late increase in benthic $\delta^{13}C$ [*Gebhardt et al.*, 2008; *Lund et al.*, 2011].

The $\delta^{18}O$ signal at the Brazil Margin has important implications for the use of $\delta^{18}O$ as a stratigraphic tool. As discussed by *Waelbroeck et al.* [2011], the depth-dependent timing of the deglacial shift in $\delta^{18}O$ precludes its use for millennial-scale correlations during glacial terminations. At the deep Brazil Margin sites, the primary decrease in benthic $\delta^{18}O$ occurs after 15 kyr B.P. (Figure 10). At mid-depths, however, the $\delta^{18}O$ shift began at 17 kyr B.P. or earlier (Figure 10). An assumption of $\delta^{18}O$ synchroneity across a range of water depths, even at same geographic location, would therefore introduce age errors of 2 kyr or more.

Our results also suggest that correcting benthic $\delta^{18}O$ for changes in global ice volume will likely create spurious results. For example, if one were to correct the Brazil Margin $\delta^{18}O$ record at 2950 m, it would give the impression that either local $\delta^{18}O_w$ increased or that water temperature decreased early in the deglaciation whereas the more plausible explanation is a lagged response to ice volume. If meltwater did not immediately influence the deep Atlantic, then the low $\delta^{18}O_w$ signal would have disproportionately influenced sites above

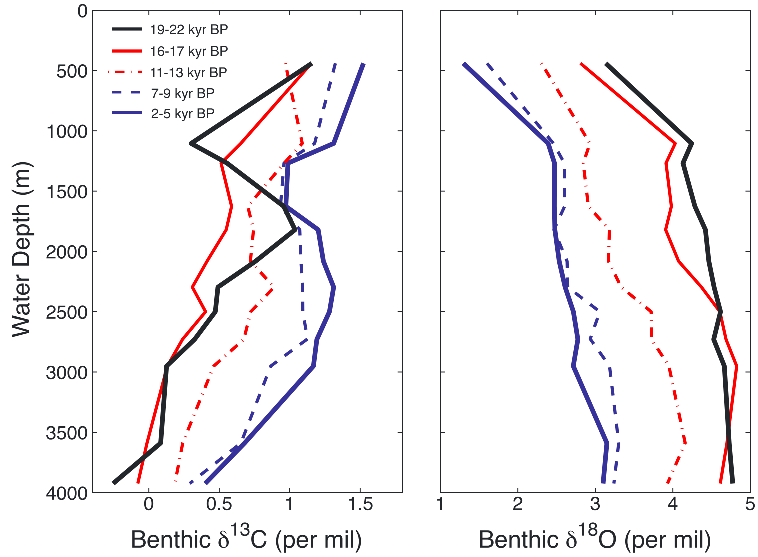

Figure 7. Vertical profiles of (left) $\delta^{13}C$ and (right) $\delta^{18}O$ for the Brazil Margin spanning the LGM to late Holocene. For clarity, profiles from each 1 kyr interval were averaged to create representative profiles for the LGM (19–23 kyr B.P.), HS1 (16–17 kyr B.P.), late deglaciation (11–13 kyr B.P.), early Holocene (7–9 kyr B.P.), and late Holocene (2–5 kyr B.P.). (left) The LGM $\delta^{13}C$ data (black line) display the influence of Glacial Antarctic Intermediate Water (GAAIW) at ~1000 m water depth, Glacial North Atlantic Intermediate Water (GNAIW) at ~1800 m, and Glacial Antarctic Bottom Water (GAABW) in the deepest portion of the profile. During HS1 (red line), $\delta^{13}C$ decreased or remained constant at all depths below 1300 m. (right) The LGM benthic $\delta^{18}O$ profile (black line) monotonically increases with water depth whereas the deglacial profiles delineate a more abrupt water mass boundary near 2300 m. Beginning during HS1 (red line), the $\delta^{18}O$ profile shows an ^{18}O-depleted and/or warmer water mass from 1300 m to 2300 m that persists into the early Holocene. During HS1, $\delta^{18}O$ remained largely unchanged below 2500 m.

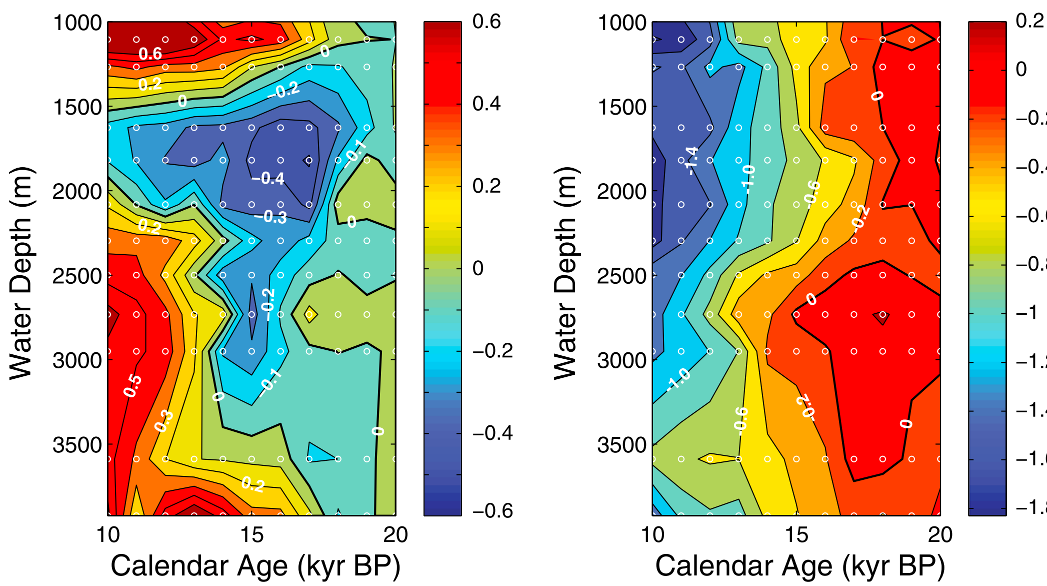

Figure 8. Hovmöller diagrams of benthic $\delta^{13}C$ and $\delta^{18}O$ anomalies for the 10–20 kyr B.P. time interval. Anomalies are the stable isotope value at each water depth minus the mean LGM value (19–23 kyr B.P.) at that depth. (left) Benthic $\delta^{13}C$ anomalies show the mid-depth negative excursion and a concurrent positive anomaly at ~1000 m. The mid-depth negative excursion occurs well before positive anomalies deeper in the water column. (right) Benthic $\delta^{18}O$ anomalies show the presence of ^{18}O-enriched water mass below 2500 m from the LGM to ~15 kyr B.P.

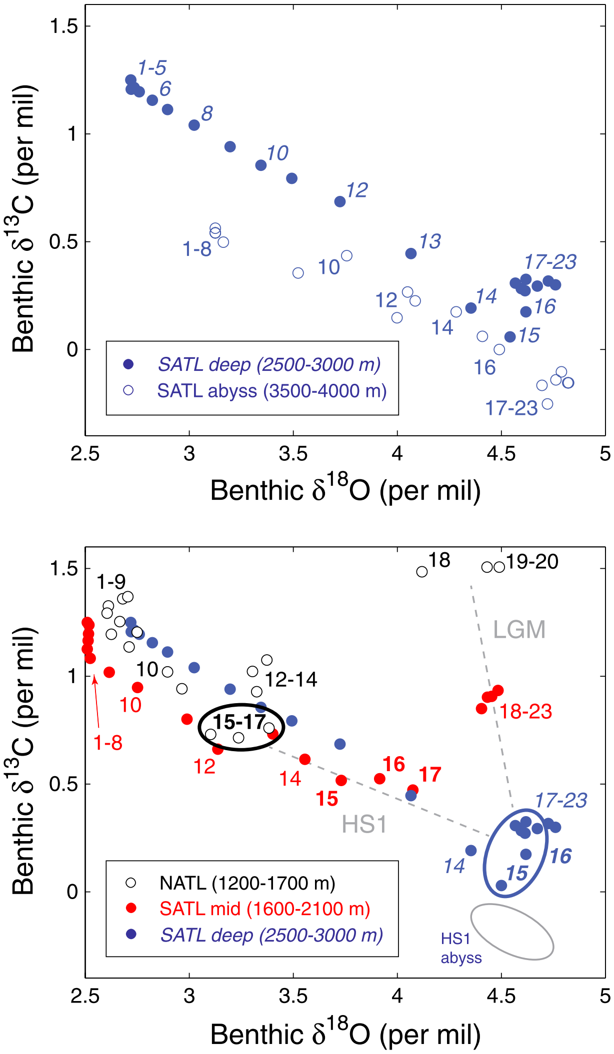

Figure 9. Crossplots of benthic δ^{18}O and δ^{13}C spanning 23 kyr B.P. to 1 kyr B.P.. All of the data are based on unsmoothed time series interpolated at 1 kyr intervals. (top) Results for the deep SW Atlantic (filled blue circles) and abyssal SW Atlantic (open blue circles) show two isotopically distinct water masses. (bottom) Data for the deep SW Atlantic (filled blue circles), mid-depth SW Atlantic (filled red circles), and upper North Atlantic (open black circles). During HS1, the mid-depth Brazil Margin data fall between North Atlantic (NATL) (black ellipse) and deep Brazil Margin end-members (blue ellipse). The mid-depth results do not fall on a mixing line between the NATL and abyssal Brazil Margin end-member (grey ellipse).

2000 m water depth. As a result, efforts to adjust shallower records for ice volume will likely undercorrect for meltwater and yield artificially large increases in temperature. Given these complications, the most reliable way to determine the effect of ice volume on benthic foraminiferal records will be to isolate $\delta^{18}O_w$ using paired δ^{18}O and temperature analyses.

4.2. Evolution of the Mid-Depth SW Atlantic

The late change in the deep SW Atlantic records informs our understanding of anomalies at mid-depth. As discussed in *Tessin and Lund* [2013], records from 1600 to 2100 m display an abrupt decrease in δ^{13}C beginning at approximately 18 kyr B.P. The negative carbon isotope excursion precedes any positive shift deeper in the water column, eliminating the abyssal SW Atlantic as a possible source. If the abyssal Atlantic was not the source of the mid-depth anomalies, then what was? Using data from the upper North Atlantic and abyssal southwest Atlantic, *Tessin and Lund* [2013] argued that the mid-depth results were inconsistent with mixing between NCW and abyssal SCW. The new data from cores 63GGC and 20JPC, however, indicate that the deep southwest Atlantic (2500–3000 m) was isotopically distinct from the abyss (3500–4000 m) (Figure 9, top). While both depth horizons had a similar δ^{18}O (~4.7‰), δ^{13}C in the deep SW Atlantic was ~0.4‰ higher. Sites above 2500 m would therefore be influenced by a water mass with higher δ^{13}C than originally inferred.

Figure 9 (bottom) shows the time evolution of δ^{18}O-δ^{13}C pairs for the deep southwest Atlantic (blue circles), the mid-depth Southwest Atlantic (red circles), and the subpolar North Atlantic (open circles). During the LGM, the mid-depth Brazil Margin data fall on a mixing line between the abyssal Brazil Margin and the North Atlantic results, as discussed by *Tessin and Lund* [2013]. During HS1, however, the mid-depth results fall on a mixing line between the deep South Atlantic and subpolar North Atlantic data. This finding is insensitive to the choice of data used to define North Atlantic δ^{18}O and δ^{13}C during HS1. If instead we use data from all five cores in Table 4, the resulting mean HS1 values would be 3.1 ± 0.1‰ (1σ) for δ^{18}O and 0.7 ± 0.1‰ (1σ) for δ^{13}C. Using the interval of minimum δ^{13}C in each core makes little difference (3.0 ± 0.2‰ for δ^{18}O and 0.6 ± 0.05‰ for δ^{13}C). These estimates are within error of those determined by *Oppo et al*. [2015] using a different combination of high-resolution North Atlantic cores. It therefore appears that the negative δ^{13}C anomalies at the Brazil Margin can be accounted for by mixing between two water masses, one from the upper North Atlantic and the other from

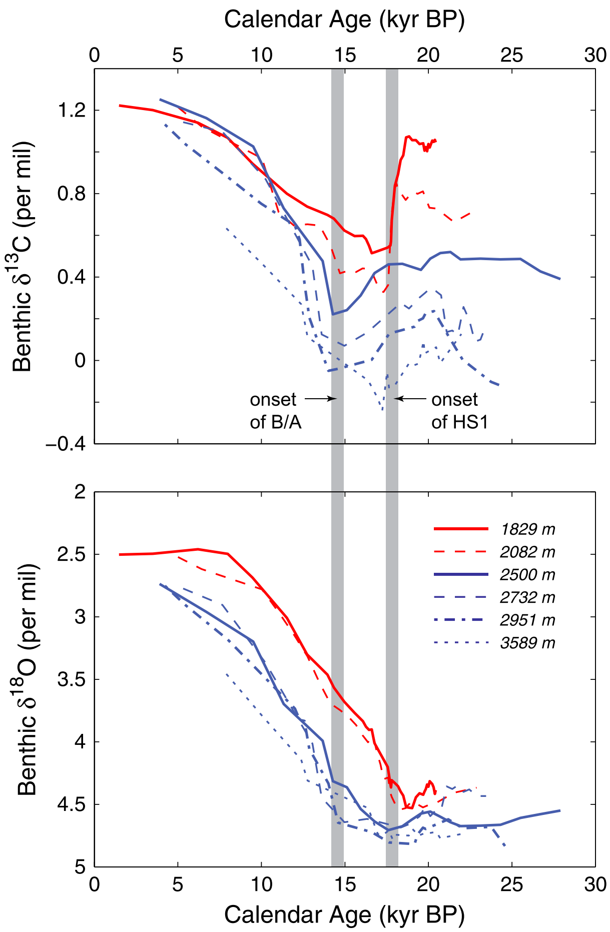

Figure 10. (top) Benthic $\delta^{13}C$ time series for the Brazil Margin spanning 1800 m to 3600 m water depth. Each record was smoothed using three-point running mean to emphasize long-term trends. The negative carbon isotope excursion at mid-depths starts at 2000 m water depth and eventually penetrates to 3000 m. (bottom) Same as Figure 10 (top) except for benthic $\delta^{18}O$. At the mid-depth sites, benthic $\delta^{18}O$ begins to decrease at 18 kyr B.P., with the deeper sites lagging by 2–4 kyr.

the deep southwest Atlantic. Because $\delta^{13}C$ and $\delta^{18}O$ in the deep southwest Atlantic were largely stable during the LGM and HS1, the $\delta^{13}C$ signal at mid-depth must have been due to the influence of NCW.

The continued influence of NCW at the Brazil Margin implies that its flux remained a substantial fraction of the LGM value. Because benthic $\delta^{18}O$ is a conservative tracer and it had a large north-south gradient during HS1 (~1.5‰), it can be used to assess the relative influence of NCW versus SCW at the Brazil Margin. During the LGM, NCW accounted for 73% of the isotopic signal at 1800 m water depth and 42% at 2300 m (Table 5a). By comparison, the HS1 proportions ranged from 52% to 35% (Table 5b). The influence of NCW therefore decreased approximately 20%, consistent with evidence for weakening of the Atlantic meridional overturning circulation (AMOC) during HS1 [*Praetorius et al.*, 2008; *Gherardi et al.*, 2009] but not a complete shutdown [*McManus et al.*, 2004]. The $\delta^{18}O$ results imply that NCW continued to affect the Brazil Margin and that the majority of the $\delta^{13}C$ signal was driven by changes in the NCW end-member rather than a large reduction in the AMOC. Alternatively, along isopycnal diffusion could have transmitted the low $\delta^{13}C$ signal from the North Atlantic in the absence of robust advection. This scenario is consistent with simulations of AMOC collapse that yield substantial $\delta^{13}C$ anomalies in the South Atlantic [*Schmittner and Lund*, 2015].

The HS1 $\delta^{18}O$ signal at mid-depths was either caused by an input of meltwater, warmer temperatures, or some combination of the two. Benthic Mg/Ca data from two subpolar North Atlantic sites suggest that temperatures at 1–1.5 km water depth increased approximately 3°C during HS1 [*Marcott et al.*, 2011]. If these data are representative of the broader North Atlantic, then more than half of the 1‰ $\delta^{18}O$ signal could be attributed to temperature. It is important to note, however, that the Mg/Ca data in the HS1 interval are based on multiple *Cibicidoides* species and the associated calibration curve is defined primarily by sites with temperatures >5°C [*Elderfield et al.*, 2006]. The relative contributions of temperature and meltwater to the $\delta^{18}O$ signal therefore remain uncertain. Nevertheless, the influence of a warm and/or ^{18}O-depleted water mass is evident in benthic $\delta^{18}O$ at the Brazil Margin from 1300 to 2300 m water depth, spanning the time interval from 17 to 8 kyr B.P. (Figure 7). The depth range of this water mass is similar to that noted in the North Atlantic [*Waelbroeck et al.*, 2011].

Taking into account the vertical profiles of $\delta^{13}C$ and $\delta^{18}O$ from the Brazil Margin and our best estimates for NCW, we are able to trace the negative carbon isotopic excursion at mid-depths to the North Atlantic rather than the Southern Ocean. We speculate that the signal was transmitted from the North Atlantic to the South Atlantic and then entrained in the Antarctic Circumpolar Current where eventually it was upwelled along isopycnals into the surface Southern Ocean [*Marshall and Speer*, 2012]. Entrainment into

Table 5a. Stable Isotope Values and Proportions of Northern Component Water (NCW) at Three Brazil Margin Mid-Depth Sites During the LGM[a]

Water Depth (m)	LGM Mean $\delta^{18}O$ (‰)	SE	$\delta^{18}O$-Based Fraction NCW	Error	LGM Mean $\delta^{13}C$ (‰)	SE	$\delta^{13}C$-Based Fraction NCW	Error
1820	4.39	0.02	**0.70**	0.22	1.04	0.04	**0.73**	0.12
2082	4.49	0.03	**0.56**	0.20	0.76	0.09	**0.56**	0.11
2296	4.58	0.04	**0.42**	0.19	0.55	0.10	**0.43**	0.10

[a]Proportions for the LGM are based NCW end-member values of $\delta^{18}O = 4.2 \pm 0.1$‰ and $\delta^{13}C = 1.5 \pm 0.1$‰ [*Curry and Oppo*, 2005] and southern component end-member values of $\delta^{18}O$ of 4.85 ± 0.1‰ and $\delta^{13}C = -0.2 \pm 0.2$‰ [*Hoffman and Lund*, 2012]. The errors for the $\delta^{13}C$-based LGM proportions are smaller because of the large contrast in $\delta^{13}C$ between northern and southern end-members.

Sub-Antarctic Mode Water would then carry the signal back to the Brazil Margin where it would be recorded at shallower depths. The timing of the deglacial benthic Brazil Margin $\delta^{13}C$ shift at 440 m is consistent with such a scenario (Figure 4). At 440 m, $\delta^{13}C$ decreased beginning at approximately 16 kyr B.P., well after the mid-depth anomaly. Alternatively, the signal at 440 m coincides with a positive $\delta^{13}C$ shift in the abyss (Figure 8), implying that the two signals may have be linked by upwelling of ^{13}C-depleted water in the Southern Ocean and subsequent northward advection by mode waters [*Spero and Lea*, 2002].

4.3. Drivers of Northern Component Variability

What was the driver of the $\delta^{18}O$ signal in the North Atlantic? *Dokken and Jansen* [1999] argue that coherent planktonic and benthic $\delta^{18}O$ signals in the Nordic Seas during Heinrich stadial events were due to the formation of brines that transmitted a low $\delta^{18}O$ meltwater signal from the surface to mid-depth. Subsequent work, however, suggests that much of the Heinrich stadial $\delta^{18}O$ signal was driven by warming, inconsistent with the brine mechanism [*Marcott et al.*, 2011]. Subsurface warming may be triggered by weakening of the AMOC [*Ruhlemann et al.*, 2004]; a simulated 70% decrease in AMOC strength yields subsurface temperature anomalies broadly consistent with those estimated using benthic foraminiferal Mg/Ca [*Marcott et al.*, 2011]. Although early Pa/Th results were consistent with a shutdown of the AMOC during HS1 [*McManus et al.*, 2004], data from shallower in the water column show that Pa continued to be exported out the North Atlantic above 2000 m [*Gherardi et al.*, 2009]. The Brazil Margin data presented here also imply that NCW continued to influence the South Atlantic. If the AMOC was substantially weaker during HS1, then it could account for much of the North Atlantic $\delta^{18}O$ signal. If this was not the case, then another mechanism would be required to explain the observed warming.

The source of negative carbon isotopic excursions in the North Atlantic has also been enigmatic. Given that a southern source for the anomalies seems implausible, the signal must instead be driven by processes in the North Atlantic. Exchange with a ^{13}C-depleted atmosphere is an unlikely explanation given that the $\delta^{13}C$ anomaly in many parts of the North Atlantic was at least twice the atmospheric signal during HS1. Alternatively, enhanced stratification due to meltwater input may have limited air-sea gas exchange and yielded lower oceanic $\delta^{13}C$ and $\Delta^{14}C$ [*Waelbroeck et al.*, 2011]. As a consequence, we would expect the atmosphere to display the opposite behavior, but instead both atmospheric $\delta^{13}C$ [*Schmitt et al.*, 2012] and $\Delta^{14}C$ [*Southon et al.*, 2012] decreased during HS1. B/Ca results from V28-122 in the tropical North Atlantic also show that $[CO_3^{2-}]$

Table 5b. Stable Isotope Values and Proportions of NCW at Three Brazil Margin Mid-Depth Sites During HS1[a]

Water Depth (m)	HS1 Mean $\delta^{18}O$ (‰)	SE	HS1 Fraction NCW	Error	Change relative to LGM (%)
1820	3.84	0.03	**0.52**	0.10	−27
2082	3.95	0.04	**0.45**	0.10	−19
2296	4.10	0.07	**0.35**	0.09	−17

[a]Proportions for HS1 are based on a NCW $\delta^{18}O$ of 3.1 ± 0.2‰ and a southern component $\delta^{18}O$ of 4.65 ± 0.1‰ (Figure 9). Only $\delta^{18}O$ was used to determine HS1 fractions because of the large interbasin $\delta^{18}O$ contrast at mid-depths compared to $\delta^{13}C$. Note that the fraction NCW results are only weakly sensitive to end-member uncertainty because of the large contrast in end-member $\delta^{18}O$ values (~1.5‰).

decreased in step with the $\delta^{13}C$ decline at mid-depths [*Yu et al*., 2010; *Oppo and Fairbanks*, 1989]. Assuming that alkalinity remained approximately constant, the data suggest that dissolved inorganic carbon increased during HS1, opposite the expected pattern if air-sea gas exchange was curtailed. Additional B/Ca records are necessary to determine whether the initial data from V28-122 are representative of the broader North Atlantic.

Another possibility is that enhanced export of ^{13}C-depleted carbon from surface waters and remineralization at depth could have produced lower NCW $\delta^{13}C$ values. Such a process would tend to increase the vertical $\delta^{13}C$ gradient in the upper North Atlantic, however a pattern that appears to be inconsistent with available HS1 $\delta^{13}C$ data [*Oppo and Curry*, 2012]. A full test of the biological-pump mechanism will require detailed planktonic $\delta^{13}C$ records from a range of latitudes in the North Atlantic. Given the data in hand, however, neither decreased air-sea gas exchange nor enhanced biological productivity appears to be feasible explanations.

The most likely cause of the abrupt carbon isotope excursions is weakening of the AMOC. Although direct evidence for AMOC cessation during HS1 remains controversial [*McManus et al*., 2004; *Keigwin and Boyle*, 2008; *Gherardi et al*., 2009; *Lippold et al*., 2009], an overall weakening would limit input of high ^{13}C water from the surface ocean and therefore create negative carbon isotope anomalies at depth [*Zahn et al*., 1997; *Praetorius et al*., 2008]. A reduction in preformed $\delta^{13}C$ of NCW would also explain the larger HS1 $\delta^{13}C$ signal in the North Atlantic relative to the Brazil Margin. Additionally, results from an intermediate complexity model suggest that a collapse in the AMOC increases the residence time of deep water in the North Atlantic, allowing for the accumulation of ^{13}C-depleted respired carbon [*Schmittner and Lund*, 2015]. The combined effect of changes in preformed $\delta^{13}C$ and regenerated $\delta^{13}C$ yields a strong meridional gradient in $\delta^{13}C$ anomalies, similar to the observed pattern. The magnitude of the modeled $\delta^{13}C$ signal is somewhat larger than observed, however, suggesting that a complete shutdown did not occur. Such a scenario also appears to be inconsistent with the continued influence of northern component water at the Brazil Margin.

Radiocarbon provides another line of evidence for constraining the Atlantic circulation during HS1. Data from the South Iceland Rise imply that $\Delta^{14}C$ at ~2 km water depth was ~500‰ lower than the atmosphere during HS1 [*Thornalley et al*., 2011]. These results were initially explained by invoking low $\Delta^{14}C$ southern component water but the lack of similarly large $\Delta^{14}C$ anomalies at sites further south makes this scenario unlikely [*Robinson et al*., 2005; *Cleroux et al*., 2011; *Sortor and Lund*, 2011; *Burke and Robinson*, 2012]. As for the $\delta^{13}C$ signal, the source of ^{14}C-depleted carbon appears to be endemic to the North Atlantic.

Results from the Brazil Margin support the notion that mid-depth waters were ^{14}C-depleted during the deglaciation. The difference in $\Delta^{14}C$ between 1800 m water depth and the atmosphere ($\Delta\Delta^{14}C$) was approximately −200‰ during HS1 (Figure 5). Compared to the expected $\Delta\Delta^{14}C$ of −130‰, this represents a $\Delta^{14}C$ decrease of ~70‰. Coral-based estimates from a similar depth range in the western North Atlantic yield $\Delta\Delta^{14}C$ values of −150‰ to −250‰ during HS1 [*Robinson et al*., 2005], an even larger shift relative to the modern value of −100‰ [*Stuiver and Ostlund*, 1980]. Thus, there appears to be a north-south gradient in the radiocarbon signal in the western Atlantic, consistent with a change driven by northern component water. The larger $\Delta\Delta^{14}C$ signal at the Brazil Margin later in the deglaciation (Figure 5) may reflect input of ^{14}C-depleted water from the Southern Ocean, where decreased stratification and upward mixing of ^{14}C-depleted water likely influenced UCDW $\Delta^{14}C$ after 15 kyr B.P. [*Burke and Robinson*, 2012]. Diagnosing the ultimate source of the carbon isotope anomalies will require additional $\Delta^{14}C$ and carbonate ion records from both the North and South Atlantic. Modeling of AMOC influence on the $\delta^{13}C$, $\delta^{18}O$, and $\Delta^{14}C$ tracer fields will also be necessary to determine if the timing and magnitude of the reconstructed anomalies can be entirely attributed to a change in circulation or whether additional processes were involved.

5. Conclusions

The decrease in $\delta^{13}C$ of atmospheric CO_2 early in the last deglaciation may have been driven by outgassing from a ^{13}C-depleted oceanic reservoir [*Tschumi et al*., 2011]. Given that the deep South Atlantic was characterized by low $\delta^{13}C$ during the LGM, it is a logical choice to explore. Here we evaluate the likelihood of this scenario by synthesizing 12 benthic stable isotopic records from the Brazil Margin that span 400 m to 4000 m water depth. The records are placed in an internally consistent chronologic framework that spans the time interval from the LGM to late Holocene. Despite evidence for age reversals in the cores, we find that four separate sites below 2300 m remained ^{13}C depleted and ^{18}O enriched until 15 kyr B.P. or later. Given that both $\delta^{13}C$ and $\delta^{18}O$ are circulation tracers, the data are inconsistent with an invigorated abyssal ocean circulation that would have liberated ^{13}C-depleted carbon from the abyss. Instead, the primary changes in $\delta^{13}C$ and $\delta^{18}O$ occurred after 15 kyr B.P., implying that the abyssal South Atlantic may have contributed to the second rise in atmospheric CO_2 later in the deglaciation.

New benthic stable isotopic records from 2730 m and 2950 m water depth indicate that the deep SW Atlantic was isotopically distinct from the abyss during HS1. As a result, we find that mid-depth $\delta^{13}C$ anomalies can be explained by mixing between deep southern component and northern component water. Stable $\delta^{13}C$ and $\delta^{18}O$ values in the deep Southwest Atlantic imply that the mid-depth signal was driven by a change in NCW. The continued influence of NCW at the Brazil Margin during HS1 appears to be inconsistent with a complete cessation of the AMOC, unless along isopycnal mixing rapidly transmitted low $\delta^{18}O$ and $\delta^{13}C$ signals from the North to the South Atlantic.

Vertical profiles of $\delta^{18}O$ show that the Brazil Margin was characterized by a strong vertical gradient in $\delta^{18}O$ from 2000 to 2500 m water depth throughout the deglaciation. The early decrease in $\delta^{18}O$ in the upper part of the water column is consistent with input of ^{18}O-depleted glacial meltwater into the North Atlantic and the advection and/or diffusion of the signal to the Brazil Margin. The strong vertical gradient in $\delta^{18}O$ disappeared by 7 kyr B.P., the approximate time of global sea level stabilization. The depth dependent timing in the $\delta^{18}O$ signal argues against the use of ice volume corrections during glacial terminations. Below 2500 m, the primary decrease in benthic $\delta^{18}O$ occurs after 15 kyr B.P., whereas at mid-depths the $\delta^{18}O$ shift began at 17 kyr B.P. or earlier. Assuming that $\delta^{18}O$ synchroneity could therefore introduce age errors of ~2 kyr or more and yield spurious hydrographic interpretations. Adjusting the deep records for ice volume would incorrectly suggest that either $\delta^{18}O_w$ increased or that water temperature decreased early in the deglaciation. The lack of an $\delta^{18}O$ signal in the deep South Atlantic also implies that low $\delta^{18}O_w$ meltwater would have disproportionately influenced sites above 2000 m. Efforts to adjust shallower records for ice volume will therefore tend to undercorrect for meltwater and yield artificially large increases in temperature.

Benthic $\Delta^{14}C$ results from the Brazil Margin suggest that either the mid-depth South Atlantic was more poorly ventilated during the deglaciation or that $\Delta^{14}C$ of northern component water decreased. A change in southern component $\Delta^{14}C$ is an unlikely factor given the overall stability in deep southern component $\delta^{18}O$ and $\delta^{13}C$ during HS1. Instead, $\Delta^{14}C$ variability in the North Atlantic appears to be the primary driver of the Brazil Margin signal. A large $\Delta^{14}C$ anomaly later in the deglaciation may reflect the influence of ^{14}C-depleted carbon from the Southern Ocean.

The overall pattern in the Brazil Margin records is one of early changes at mid-depth followed by variability in the deeper part in the water column. The data are inconsistent with a change in the abyssal South Atlantic circulation early in the deglaciation. Instead, northern component variability was the most likely driver of the mid-depth anomalies. Detailed data and modeling intercomparison studies will be necessary to determine whether changes in AMOC strength can feasibly account for stable isotope and radiocarbon tracer fields in the Atlantic basin. Given the similarity between mid-depth Atlantic $\delta^{13}C$ records and atmospheric $\delta^{13}C$ during the last deglaciation, isolating the driver of the oceanic anomalies will be key to understanding the rise in atmospheric CO_2 during the last deglaciation.

Acknowledgments
We would like to thank Lora Wingate for her help with stable isotope analyses. We would also like to thank Rachel Franzblau, Rachel Seltz, and Elliot Jackson for sample processing. We are grateful to the WHOI core laboratory for sample collection and to Bill Curry and Delia Oppo for having the foresight to collect the Brazil Margin cores. We would like to additionally thank Delia Oppo for providing three dates for core KNR159-5-90GGC and for providing valuable feedback on this work. Data presented in this paper are available on the NOAA Paleoclimatology Data website (http://www.ncdc.noaa.gov/data-access/paleoclimatology-data). This work was supported by NSF grant OCE-1003500 and the NSF Graduate Research Fellowship Program (A. Tessin).

References

Adkins, J. F., K. McIntyre, and D. P. Schrag (2002), The salinity, temperature, and delta O-18 of the glacial deep ocean, *Science*, *298*(5599), 1769–1773.

Anderson, R. F., S. Ali, L. I. Bradtmiller, S. H. H. Nielsen, M. Q. Fleisher, B. E. Anderson, and L. H. Burckle (2009), Wind-driven upwelling in the Southern Ocean and the deglacial rise in atmospheric CO2, *Science*, *323*(5920), 1443–1448.

Angulo, R. J., M. C. de Souza, P. J. Reimer, and S. K. Sasaoka (2005), Reservoir effect of the southern and southeastern Brazilian coast, *Radiocarbon*, *47*(1), 67–73.

Broecker, W. S. (1982), Ocean chemistry during glacial time, *Geochim. Cosmochim. Acta*, *46*(10), 1689–1705.

Burke, A., and L. F. Robinson (2012), The Southern Ocean's role in carbon exchange during the last deglaciation, *Science*, *335*(6068), 557–561.

Clark, P. U., A. S. Dyke, J. D. Shakun, A. E. Carlson, J. Clark, B. Wohlfarth, J. X. Mitrovica, S. W. Hostetler, and A. M. McCabe (2009), The Last Glacial Maximum, *Science*, *325*(5941), 710–714.

Cleroux, C., P. Demenocal, and T. Guilderson (2011), Deglacial radiocarbon history of tropical Atlantic thermocline waters: Absence of CO_2 reservoir purging signal, *Quat. Sci. Rev.*, *30*(15–16), 1875–1882.

Curry, W. B., and D. W. Oppo (2005), Glacial water mass geometry and the distribution of delta C-13 of Sigma CO_2 in the western Atlantic Ocean, *Paleoceanography*, *20*, PA1017, doi:10.1029/2004PA001021.

Curry, W. B., J. C. Duplessy, L. D. Labeyrie, and N. J. Shackleton (1988), Changes in the distribution of d13C of deep water CO_2 between the last glaciation and Holocene, *Paleoceanography*, *3*, 317–341, doi:10.1029/PA003i003p00317.

Cutler, K. B., R. L. Edwards, F. W. Taylor, H. Cheng, J. Adkins, C. D. Gallup, P. M. Cutler, G. S. Burr, and A. L. Bloom (2003), Rapid sea-level fall and deep-ocean temperature change since the last interglacial period, *Earth Planet. Sci. Lett.*, *206*(3–4), 253–271.

Dokken, T. M., and E. Jansen (1999), Rapid changes in the mechanism of ocean convection during the last glacial period, *Nature*, *401*(6752), 458–461.

Duplessy, J. C., N. J. Shackleton, R. G. Fairbanks, L. Labeyrie, D. Oppo, and N. Kallel (1988), Deep water source variations during the last climatic cycle and their impact on the global deep water circulation, *Paleoceanography*, *3*, 343–360.

Elderfield, H., J. Yu, P. Anand, T. Kiefer, and B. Nyland (2006), Calibrations for benthic foraminiferal Mg/Ca paleothermometry and the carbonate ion hypothesis, *Earth Planet. Sci. Lett.*, *250*(3–4), 633–649.

Gebhardt, H., M. Sarnthein, P. M. Grootes, T. Kiefer, H. Kuehn, F. Schmieder, and U. Rohl (2008), Paleonutrient and productivity records from the subarctic North Pacific for Pleistocene glacial terminations I to V, *Paleoceanography*, *23*, PA4212, doi:10.1029/2007PA001513.

Gherardi, J. M., L. Labeyrie, S. Nave, R. Francois, J. F. McManus, and E. Cortijo (2009), Glacial-interglacial circulation changes inferred from Pa-231/Th-230 sedimentary record in the North Atlantic region, *Paleoceanography*, *24*, PA2204, doi:10.1029/2008PA001696.

Herguera, J. C., T. Herbert, M. Kashgarian, and C. Charles (2010), Intermediate and deep water mass distribution in the Pacific during the Last Glacial Maximum inferred from oxygen and carbon stable isotopes, *Quat. Sci. Rev.*, *29*(9–10), 1228–1245.

Hoffman, J. L., and D. C. Lund (2012), Refining the stable isotope budget for Antarctic Bottom Water: New foraminiferal data from the abyssal southwest Atlantic, *Paleoceanography*, *27*, PA1213, doi:10.1029/2011PA002216.

Kallel, N., L. D. Labeyrie, A. Juilletleclerc, and J. C. Duplessy (1988), A deep hydrological front between intermediate and deep-water masses in the glacial Indian Ocean, *Nature*, *333*(6174), 651–655.

Keigwin, L. D., and E. A. Boyle (2008), Did North Atlantic overturning halt 17,000 years ago?, *Paleoceanography*, *23*, PA1101, doi:10.1029/2007PA001500.

Key, R. M., A. Kozyr, C. L. Sabine, K. Lee, R. Wanninkhof, J. L. Bullister, R. A. Feely, F. J. Millero, C. Mordy, and T. H. Peng (2004), A global ocean carbon climatology: Results from Global Data Analysis Project (GLODAP), *Global Biogeochem. Cycles*, *18*, GB4031, doi:10.1029/2004GB002247.

Lippold, J., J. Grutzner, D. Winter, Y. Lahaye, A. Mangini, and M. Christl (2009), Does sedimentary Pa-231/Th-230 from the Bermuda Rise monitor past Atlantic Meridional Overturning Circulation?, *Geophys. Res. Lett.*, *36*, L12601, doi:10.1029/2009GL038068.

Lund, D. C., J. F. Adkins, and R. Ferrari (2011a), Abyssal Atlantic circulation during the Last Glacial Maximum: Constraining the ratio between transport and vertical mixing, *Paleoceanography*, *26*, PA1213, doi:10.1029/2010PA001938.

Lund, D. C., A. C. Mix, and J. Southon (2011b), Increased ventilation age of the deep northeast Pacific Ocean during the last deglaciation, *Nat. Geosci.*, *4*, 771–774.

Marcott, S. A., et al. (2011), Ice-shelf collapse from subsurface warming as a trigger for Heinrich events, *Proc. Natl. Acad. Sci. U.S.A.*, *108*(33), 13,415–13,419.

Marshall, J., and K. Speer (2012), Closure of the meridional overturning circulation through Southern Ocean upwelling, *Nat. Geosci.*, *5*, 171–180.

McManus, J. F., R. Francois, J. M. Gherardi, L. D. Keigwin, and S. Brown-Leger (2004), Collapse and rapid resumption of Atlantic meridional circulation linked to deglacial climate changes, *Nature*, *428*(6985), 834–837.

Monnin, E., A. Indermuhle, A. Dallenbach, J. Fluckiger, B. Stauffer, T. F. Stocker, D. Raynaud, and J. M. Barnola (2001), Atmospheric CO_2 concentrations over the last glacial termination, *Science*, *291*(5501), 112–114.

Monnin, E., et al. (2004), Evidence for substantial accumulation rate variability in Antarctica during the Holocene, through synchronization of CO_2 in the Taylor Dome, Dome C and DML ice cores, *Earth Planet. Sci. Lett.*, *224*(1–2), 45–54.

Oppo, D. W., and W. B. Curry (2012), Deep Atlantic circulation during the Last Glacial Maximum and deglaciation, *Nat. Educ. Knowl.*, *3*(10), 1.

Oppo, D. W., and R. G. Fairbanks (1989), Carbon isotope composition of tropical surface water during the past 22,000 years, *Paleoceanography*, *4*, 333–351, doi:10.1029/PA004i004p00333.

Oppo, D. W., W. B. Curry, and J. McManus (2015), What do benthic $\delta^{13}C$ and $\delta^{18}O$ data tell us about Atlantic circulation during Heinrich Stadial 1?, *Paleoceanography*, doi:10.1002/2014PA002667.

Ostermann, D. R., and W. B. Curry (2000), Calibration of stable isotopic data: An enriched delta O-18 standard used for source gas mixing detection and correction, *Paleoceanography*, *15*, 353–360, doi:10.1029/1999PA000411.

Parrenin, F., V. Masson-Delmotte, P. Kohler, D. Raynaud, D. Paillard, J. Schwander, C. Barbante, A. Landais, A. Wegner, and J. Jouzel (2013), Synchronous change of atmospheric CO2 and Antarctic temperature during the last deglacial warming, *Science*, *339*(6123), 1060–1063.

Peck, V. L., I. R. Hall, R. Zahn, H. Elderfield, F. Grousset, S. R. Hemming, and J. D. Scourse (2006), High resolution evidence for linkages between NW European ice sheet instability and Atlantic meridional overturning circulation, *Earth Planet. Sci. Lett.*, *243*(3–4), 476–488.

Praetorius, S. K., J. F. McManus, D. W. Oppo, and W. B. Curry (2008), Episodic reductions in bottom-water currents since the last ice age, *Nat. Geosci.*, *1*(7), 449–452.

Reimer, P. J., et al. (2013), Intcal13 and marine13 radiocarbon age calibration curves 0-50,000 years cal BP, *Radiocarbon*, *55*(4), 1869–1887.

Rickaby, R. E. M., and H. Elderfield (2005), Evidence from the high-latitude North Atlantic for variations in Antarctic Intermediate water flow during the last deglaciation, *Geochem. Geophys. Geosyst.*, *6*, Q05001, doi:10.1029/2004GC000858.

Robinson, L. F., J. F. Adkins, L. D. Keigwin, J. Southon, D. P. Fernandez, S. L. Wang, and D. S. Scheirer (2005), Radiocarbon variability in the western North Atlantic during the last deglaciation, *Science*, *310*(5753), 1469–1473.

Ruhlemann, C., S. Mulitza, G. Lohmann, A. Paul, M. Prange, and G. Wefer (2004), Intermediate depth warming in the tropical Atlantic related to weakened thermohaline circulation: Combining paleoclimate data and modeling results for the last deglaciation, *Paleoceanography*, *19*, PA1025, doi:10.1029/2003PA000948.

Schlitzer, R. (2000), Ellectronic atlas of WOCE hydrographic and tracer data now available, *Eos Trans. AGU*, *81*(5), 45–45, doi:10.1029/00EO00028.

Schmitt, J., et al. (2012), Carbon isotope constraints on the deglacial CO_2 rise from ice cores, *Science*, *336*(6082), 711–714.

Schmittner, A., and D. C. Lund (2015), Early deglacial Atlantic overturning decline and its role in atmospheric CO2 rise inferred from carbon isotopes (δ13C), *Clim. Past*, *1*, 135–152, doi:10.5194/cp-11-135-2015.

Shakun, J. D., P. U. Clark, F. He, S. A. Marcott, A. C. Mix, Z. Y. Liu, B. Otto-Bliesner, A. Schmittner, and E. Bard (2012), Global warming preceded by increasing carbon dioxide concentrations during the last deglaciation, *Nature*, *484*(7392), 49–54.

Sigman, D. M., and E. A. Boyle (2000), Glacial/interglacial variations in atmospheric carbon dioxide, *Nature*, *407*(6806), 859–869.

Slowey, N. C., and W. B. Curry (1995), Glacial-interglacial differences in circulation and carbon cycling within the upper western North-Atlantic, *Paleoceanography*, *10*, 715–732, doi:10.1029/95PA01166.

Sortor, R. N., and D. C. Lund (2011), No evidence for a deglacial intermediate water Delta C-14 anomaly in the SW Atlantic, *Earth Planet. Sci. Lett.*, *310*(1–2), 65–72.

Southon, J., A. L. Noronha, H. Cheng, R. L. Edwards, and Y. J. Wang (2012), A high-resolution record of atmospheric C-14 based on Hulu Cave speleothem H82, *Quat. Sci. Rev.*, *33*, 32–41.

Spero, H. J., and D. W. Lea (2002), The cause of carbon isotope minimum events on glacial terminations, *Science*, *296*(5567), 522–525.

Stern, J. V., and L. E. Lisiecki (2013), North Atlantic circulation and reservoir age changes over the past 41,000 years, *Geophys. Res. Lett.*, *40*, 3693–3697, doi:10.1002/grl.50679.

Stuiver, M., and H. G. Ostlund (1980), Geosecs Atlantic radiocarbon, *Radiocarbon*, *22*, 1–24.

Tessin, A. C., and D. C. Lund (2013), Isotopically depleted carbon in the mid-depth South Atlantic during the last deglaciation, *Paleoceanography*, *28*, 296–306, doi:10.1002/palo.20026.

Thompson, W. G., and S. L. Goldstein (2006), A radiometric calibration of the SPECMAP timescale, *Quat. Sci. Rev.*, *25*(23–24), 3207–3215.

Thornalley, D. J. R., I. N. McCave, and H. Elderfield (2010), Freshwater input and abrupt deglacial climate change in the North Atlantic, *Paleoceanography*, *25*, PA1201, doi:10.1029/2009PA001772.

Thornalley, D. J. R., S. Barker, W. S. Broecker, H. Elderfield, and I. N. McCave (2011), The deglacial evolution of North Atlantic deep convection, *Science*, *331*, 202–205.

Tschumi, T., F. Joos, M. Gehlen, and C. Heinze (2011), Deep ocean ventilation, carbon isotopes, marine sedimentation and the deglacial CO_2 rise, *Clim. Past*, *7*(3), 771–800.

Veres, D., et al. (2012), The Antarctic ice core chronology (AICC2012): An optimized multi-parameter and multi-site dating approach for the last 120 thousand years, *Clim. Past Discuss.*, *8*, 6011–6049.

Waelbroeck, C., L. C. Skinner, L. Labeyrie, J. C. Duplessy, E. Michel, N. V. Riveiros, J. M. Gherardi, and F. Dewilde (2011), The timing of deglacial circulation changes in the Atlantic, *Paleoceanography*, *26*, PA3213, doi:10.1029/2010PA002007.

Yu, J. M., W. S. Broecker, H. Elderfield, Z. D. Jin, J. McManus, and F. Zhang (2010), Loss of carbon from the deep sea since the Last Glacial Maximum, *Science*, *330*(6007), 1084–1087.

Zahn, R., and A. Stuber (2002), Suborbital intermediate water variability inferred from paired benthic foraminiferal Cd/Ca and delta C-13 in the tropical West Atlantic and linking with North Atlantic climates, *Earth Planet. Sci. Lett.*, *200*(1–2), 191–205.

Zahn, R., J. Schonfeld, H. R. Kudrass, M. H. Park, H. Erlenkeuser, and P. Grootes (1997), Thermohaline instability in the North Atlantic during meltwater events: Stable isotope and ice-rafted detritus records from core SO75-26KL, Portuguese margin, *Paleoceanography*, *12*, 696–710, doi:10.1029/97PA00581.